arXiv:cond-mat/9902332v1 [cond-mat.dis-nn] 25 Feb 1999

Nucleus-Electron Model for States Changing from a Liquid Metal to a Plasma and the Saha Equation

J. Chihara and Y. Ueshima

Advanced Photon Research Center, Japan Atomic Energy Research Institute

Tokai, Ibaraki 319-1195, Japan

S. Kiyokawa

Department of Physics, Nara Women's University,

Kita-Uoya Nishimachi, Nara 630-8506, Japan

(November 20, 2018)

Abstract

We extend the quantal hypernetted-chain (QHNC) method, which has been proved to yield accurate results for liquid metals, to treat a *partially ionized* plasma. In a plasma, the electrons change from a quantum to a classical fluid gradually with increasing temperature; the QHNC method applied to the electron gas is in fact able to provide the electron-electron correlation at arbitrary temperature. As an illustrating example of this approach, we investigate how liquid rubidium becomes a plasma by increasing the temperature from 0 to 30 eV at a fixed normal ion-density $1.03\times10^{22}/\mathrm{cm}^3$. The electron-ion radial distribution function (RDF) in liquid Rb has distinct inner-core and outer-core parts. Even at a temperature of 1 eV, this clear distinction remains as

a characteristic of a liquid metal. At a temperature of 3 eV, this distinction disappears, and rubidium becomes a plasma with the ionization 1.21. The temperature variations of bound levels in each ion and the average ionization are calculated in Rb plasmas at the same time. Using the density-functional theory, we also derive the Saha equation applicable even to a high-density plasma at low temperatures. The QHNC method provides a procedure to solve this Saha equation with ease by using a recursive formula; the charge population of differently ionized species are obtained in Rb plasmas at several temperatures. In this way, it is shown that, with the atomic number as the only input, the QHNC method produces the average ionization, the electron-ion and ion-ion RDF's, and the charge population which are consistent with the atomic structure of each ion for a partially ionized plasma.

52.25.-b, 52.25.Kn, 52.25.Jm, 05.30.Fk, 61.25.Mv

Typeset using REVTEX

I. INTRODUCTION

In order to calculate thermodynamic functions, transport coefficients and optical properties in a partially ionized plasma, it is a fundamental problem to determine the average ionization $Z_{\rm I}$, the equilibrium correlations among ions and electrons, the atomic structure (bound-levels in the ions) and the charge population (ionization balance) of differently ionized species, in a self-consistent way with each other in these quantities. However, at the present stage there is no theory which can produce these quantities in a *partially ionized* plasma in a unified manner. It is the purpose of the present work to show that the quantal hypernetted-chain (QHNC) equation [1] developed for a liquid metal can be extended to calculate these quantities of a partially ionized plasma in a unified manner.

Up to the present, in the calculation of thermodynamic functions or optical properties in a partially ionized plasma, the ion-sphere (IS) model [2–7] is used as the standard method. Although there are many kinds of variations in the IS model, the essential point of this model is that the ion-ion correlation in a plasma is approximated by the step function $\theta(r-a)$ with the Wigner-Seitz radius a; an atom is considered to be either confined within the ion-sphere or immersed in the infinite jellium. It should be remarked that this model is only applicable for high-density and low-temperature systems, that is, limited to a narrow range of densities and temperatures for the plasma state.

On the basis of the density functional (DF) theory, Dharma-wardana and Perrot [8] derived a set of integral equations for static correlation functions in a strongly coupled plasma; it was shown [9] that this method breaks down when it treats a plasma with a significant number of bound electrons as an ion due to its improper treatment of the electron-ion correlation. To judge whether a theory treating a partially ionized plasma is proper or not, we have the criterion as to what extent it can reproduce the observed structure factors of liquid metals for which many reliable experimental data exist. This is a liquid metal can be taken as a special type of partially ionized plasma. In this context, we have proposed a set of integral equations for radial distribution functions (RDF) in a liquid metal as a nucleus-

electron mixture [1] on the basis of the DF theory in the quantal hypernetted-chain (QHNC) approximation. At this point, it should be kept in mind that the QHNC theory is limited to treating only a "simple" liquid metal, where the bound states are clearly distinguished from the continuum state. Already, we have applied the QHNC method to several simple liquid metals [10–14], and obtained their structure factors in excellent agreement with experiments. In these calculations, we have demonstrated that the QHNC method can determine the "outer structure" (the ion-ion and electron-ion RDF's and the ionic charge $Z_{\rm I}$) in a consistent way with the "inner structure" (the atomic structure of the ions) using the atomic number $Z_{\rm A}$ of the system as the only input data. Therefore, the QHNC method is suited for treating a plasma, where the ion-ion and electron-ion interactions may vary over a wide range in conjunction with the internal structure of each ion according to change of state condition. In a similar spirit, Perrot [15] has proposed the neutral-pseudoatom (NPA) method based on the DF theory to calculate the effective ion-ion potential for a partially ionized plasma. González *et al.* have successfully applied this theory to alkali liquids [16] and alkaline-earth liquids [17]. The NPA method can be derived from the QHNC theory with additional use of the IS approximation [9] in the determination of the pseudopotential to construct an effective ion-ion interaction. This model is called in our approach the jellium-vacancy model [11] and is used to obtain an initial guess for the effective ion-ion interaction in the iteration to solve the QHNC equation for a liquid metal. At this point, it should be recognized that the NPA method is not appropriate for treating a high-temperature plasma with the weak ion-ion correlation, since this method is based on the IS model; this fact will be discussed in the present work.

From successful applications of the QHNC method to liquid metals as mentioned before, we can expect this method constitutes an adequate representation of a partially ionized plasma. In the present work, we extend the QHNC method applicable to a plasma state, where the electrons change from a quantum fluid to a classical fluid gradually with increasing temperature; this is in contrast with a liquid metal where the electrons can be assumed to be perfectly in the Fermi degenerate state at zero temperature because of the density being

high. When the electrons in a plasma begin to behave as classical particles, it is difficult to calculate the free-electron density distribution under the external potential by solving the wave equation. Therefore, Furukawa [18] used the Thomas-Fermi (TF) approximation to evaluate the electron-ion RDF in the QHNC equation for a plasma. Also, Xu and Hansen [19] applied the TF version of the QHNC method to a hydrogen plasma with a gradient correction to the TF kinetic energy of the electrons. In the full use of the wave equation to calculate the free-electron density distribution, we demonstrate that the QHNC method can treat a partially ionized plasma by taking liquid rubidium as an illustrating example; this exhibits what changes are found when a liquid-metal turns to a plasma state with increasing temperature at a fixed ion-density. In a liquid metal, there is clear distinction between the inner-core and outer-core structures in the electron-ion RDF, which allows one to construct an electron-ion pseudopotential in a liquid metal. When a liquid metal changes into a plasma state, this distinction disappears, and we can not set up a peudopotential in the same manner as is performed in the usual liquid-metal theory.

In principle, the DF theory generates the exact density distributions of electrons and ions in a plasma. Note that it can yield only the average-ion structure in a partially ionized plasma. In a real plasma, there are many differently ionized ions around the average ion. The fundamental theory of ionization in a plasma is provided by the Saha equation. However, the usual Saha equation can be applied only to a low density equilibrium plasma, where the interactions among particles are negligible. Although there are many modifications of the Saha equation for applicability to dense plasmas by introducing the continuum lowering, any modified theory can not treat a dense plasma at low temperatures. In the present work, on the basis of the DF theory we derive the Saha equation, which provides the charge population of differently ionized ions in a dense plasma in the region from low to high temperatures; this charge population yields an average ionization consistent with an average ion in the plasma determined the DF theory. The bound levels and the chemical potential contained in the Saha equation are supplied by the QHNC equation for the ion-ion and electron-ion RDF's in the plasma. In this way, the QHNC method is shown to generate the electron-ion and

ion-ion RDF's, the average ionization $Z_{\rm I}$, and the charge population of differently ionized species to be consistent with the atomic structure (bound levels) of each ion in a unified fashion, as will be shown by the example of a rubidium plasma.

The paper is organized as follows. In §. II, we present a summary of the QHNC method along with the one-component QHNC equation for an electron gas in the jellium model, making extensions to treat a plasma. As an illustrating example, the application of this formulation to a Rb plasma is shown in § III, where the numerical technique to solve the QHNC equation is explained. In § IV, we set up the Saha equation on the basis of the DF theory, and the charge populations are calculated for Rb plasmas at a fixed liquid-metal density for several temperatures. The last section is devoted to discussion, where the limitation of the IS model is also examined, and prospects of applications based on the QHNC method are mentioned, such as calculations of the atomic structure and transport coefficients in a plasma, and the determination of the effective interactions to be used for the molecular-dynamics simulation of a plasma as a classical electron-ion mixture.

II. LIQUID METAL AND PLASMA AS NUCLEUS-ELECTRON MIXTURE

We can set up the following three models to treat liquid metals and plasmas. In the simplest model, a liquid metal can be treated as a neutral liquid, when its interatomic potential is given. However, this interatomic potential must be introduced from the outside of the model; this is impossible when treating a plasma. In the second model, a liquid metal is considered as a binary mixture of ions and electrons; in this model, the ionic charge $Z_{\rm I}$ and the electron-ion interaction are unknown except for a perfectly ionized plasma [20,8], even if the ion-ion interaction is taken as a pure Coulombic. In the case of a plasma, it is rather a fundamental problem to determine the ionization $Z_{\rm I}$. Most fundamental model is to consider a liquid metal as composed of nuclei and electrons. In this model, all input data are known beforehand if provided the atomic number $Z_{\rm A}$ of a liquid metal; this first-principles approach enable us to treat a plasma in a wide range of temperatures and densities. Therefore, let

us think of a plasma as a nucleus-electron mixture [1] consisting of $N_{\rm I}$ nuclei and $Z_{\rm A}N_{\rm I}$ electrons. Here, we single out one nucleus and fix it at the origin; then, the fixed nucleus at the origin in the mixture causes the external potentials for electrons and ions, and induces an inhomogeneous system. This inhomogeneous system can be equivalently translated into a simpler system: a fixed nucleus with the atomic number $Z_{\rm A}$ is surrounded by electrons and ions, of which structure $\rho_{\rm b}(r)$ is undetermined at first and should be determined self-consistently at final. In this simplified model, the fixed nucleus at the origin is surrounded by $(N_{\rm I}-1)$ ions interacting via a potential $v_{\rm II}(r)$ and by $Z_{\rm I}(N_{\rm I}-1)+Z_{\rm A}$ electrons. Under this circumstance, the DF theory provides effective external potentials $v_{i{\rm N}}^{\rm eff}(r)$ (i=e or I), which yield the exact electron- and ion-density distributions around the fixed nucleus on the basis of the following reference system [21]: a mixture composed of $(N_{\rm I}-1)$ noninteracting ions and $Z_{\rm I}(N_{\rm I}-1)+Z_{\rm A}$ noninteracting electrons. Each ion in the reference system is assumed to have $Z_{\rm B}$ bound-electrons with a distribution $\rho_{\rm b}(r)$. The electron-density distribution around the central nucleus is determined by solving the wave equation for noninteracting electrons in the form:

$$n_{\rm e}(r|{\rm N}) = n_{\rm e}^0(r|v_{e{\rm N}}^{\rm eff}) = n_{\rm e}^{\rm b}(r|{\rm N}) + n_{\rm e}^{\rm f}(r|{\rm N})\,, \tag{2.1}$$

under the effective external potential,

$$v_{e{\rm N}}^{\rm eff}(r) = -Z_{\rm A}e^2/r + \frac{\delta \mathcal{F}_{\rm int}}{\delta n_e(r|{\rm N})} - \mu_e^{\rm int}\,, \tag{2.2}$$

which is constructed by the DF theory in terms of the interaction part of the intrinsic free-energy $\mathcal{F}_{\rm int}$ defined from the reference system and the interaction part of the chemical potential $\mu_e^{\rm int}$. Here, $n_{\rm e}^0(r|U)$ is determined by solving the wave equation for an electron under the external potential $U(r)$ in the form:

$$n_e^0(r|U) = \Sigma_i f(\epsilon_i)|\psi_i(r)|^2\,, \tag{2.3}$$

where $\psi_i(r)$ is the wave function of the state ϵ_i (bound or free) and $f(\epsilon)$, the Fermi distribution function. Now, the density distribution $n_{\rm e}^0(r|v_{e{\rm N}}^{\rm eff})$ can be divided into two parts:

the bound- and free-electron density distributions, $n_{\rm e}^{\rm b}$ and $n_{\rm e}^{\rm f}$, respectively, according to the states ϵ_i being negative or positive.

The bound electrons $n_{\rm e}^{\rm b}(r) \equiv n_{\rm e}^{\rm b}(r|{\rm N})$ around the nucleus at the origin should be taken to constitute the ion at the origin. Therefore, unknown ion structure $\rho_{\rm b}(r)$ in the premise is determined by the condition that the central ion with $n_{\rm e}^{\rm b}(r)$ formed at the origin must be the same to any surrounding ion with the assumed structure $\rho_{\rm b}(r)$ around it, that is,

$$\rho_{\rm b}(r) = n_{\rm e}^{\rm b}(r|{\rm N})\,. \tag{2.4}$$

This leads to a self-consistent condition to determine the ion structure $\rho_{\rm b}(r)$; the central ion structure $n_{\rm e}^{\rm b}(r)$ is iteratively used as the input $\rho_{\rm b}(r)$ giving the new reference system, which determines the next effective potential (2.2) to evaluate a new $n_{\rm e}^{\rm b}(r)$. From this relation, the bound-electron number $Z_{\rm B}$ of surrounding ions can be evaluated from the bound-electron density distribution $n_{\rm e}^{\rm b}(r|{\rm N})$ by $Z_{\rm B} = \int_0^\infty n_e^{\rm b}(r) d\mathbf{r}$, that is,

$$Z_{\rm B} \equiv \sum_{i=1}^{M} \frac{g_i}{\exp[\beta(\epsilon_i - \mu_{\rm e}^0)] + 1}\,, \tag{2.5}$$

for the ion with M bound states with the degeneracy g_i, and the ionic charge is obtained by $Z_{\rm I} \equiv Z_{\rm A} - Z_{\rm B}$. In addition, the chemical potential $\mu_{\rm e}^0$ involved in Eq. (2.5) is determined by noting the fact:

$$\lim_{r\to\infty} n_{\rm e}^{\rm f}(r|{\rm I}) = \int \frac{2}{\exp[\beta(p^2/2m - \mu_{\rm e}^0)] + 1} \frac{d\mathbf{p}}{(2\pi\hbar)^3} = n_0^{\rm e} = Z_{\rm I} n_0^{\rm I}\,, \tag{2.6}$$

which can be rewritten in the form:

$$Z_{\rm A} = \sum_{i=1}^{M} \frac{g_i}{\exp[\beta(\epsilon_i - \mu_{\rm e}^0)] + 1} + \frac{1}{n_0^{\rm I}} \int \frac{2}{\exp[\beta(p^2/2m - \mu_{\rm e}^0)] + 1} \frac{d\mathbf{p}}{(2\pi\hbar)^3}\,. \tag{2.7}$$

Here, n_0^i denotes the number density of electrons or ions (i =e or I). Also, the bare ion-electron interaction is obtained from Eq. (2.2) with use of some approximations [22]:

$$v_{\rm eI}(r) \equiv -\frac{Z_{\rm A}}{r} + \int v_{\rm ee}^{\rm c}(|\mathbf{r} - \mathbf{r}'|)\, n_{\rm e}^{\rm b}(r') d\mathbf{r}' + \mu_{\rm XC}(n_{\rm e}^{\rm b}(r) + n_0^{\rm e}) - \mu_{\rm XC}(n_0^{\rm e}), \tag{2.8}$$

where $\mu_{\rm XC}(n_0^e)$ is the exchange-correlation potential in the local-density approximation.

With use of the average ionization $Z_{\rm I}$ and the bare ion-electron interaction $v_{\rm eI}(r)$, a plasma can be now modeled as a mixture of electrons and ions interacting through pair potentials $v_{ij}(r)$ [$i,j =$ e or I]. Applying the DF theory to this electron-ion mixture model, the ion-ion and electron-ion RDF's $g_{i\rm I}(r)$ are exactly expressed in terms of direct correlation functions (DCF) $C_{ij}(r)$ and bridge functions $B_{i\rm I}(r)$ as follows [1]:

$$g_{\rm eI}(r) = n_e^{0f}(r|U_{\rm e}^{\rm eff})/n_0^e \ , \tag{2.9}$$

$$g_{\rm II}(r) = \exp[-\beta U_{\rm I}^{\rm eff}(r)] \ , \tag{2.10}$$

with

$$U_{i\rm I}^{\rm eff}(r) \equiv v_{i\rm I}(r) - \Gamma_{i\rm I}(r)/\beta - B_{i\rm I}(r)/\beta \ , \tag{2.11}$$

$$\Gamma_{i\rm I}(r) \equiv \sum_l \int C_{il}(|\mathbf{r}-\mathbf{r}'|) n_0^l [g_{l\rm I}(r') - 1] d\mathbf{r}' \ . \tag{2.12}$$

Here, $n_e^{0f}(r|U_{\rm eI}^{\rm eff})$ indicates the free-electron part of the density distribution. We can see a similarity of these expressions to those of a classical binary mixture. The difference is found only in that the electron-ion RDF is determined by a wave equation in stead of the Boltzmann factor $\exp[-\beta U_{\rm e}^{\rm eff}(r)]$.

Moreover, it is shown from these expressions that the electron-ion mixture can be described as a one-component fluid interacting only via pairwise interaction $v_{\rm eff}(r)$, if the bridge function $B_{\rm II}(r)$ is taken to be the one-component bridge function. Namely, the integral equations (2.9)–(2.12) for $g_{i\rm I}(r)$ can be transformed into a set of integral equations for the one-component model of plasmas. One is an usual integral equation for the DCF $C(r)$ of a one-component fluid:

$$C(r) = \exp[-\beta v_{\rm eff}(r) + \gamma(r) + B_{\rm II}(r)] - 1 - \gamma(r) \tag{2.13}$$

with an interaction $v_{\rm eff}(r)$, and the other is an equation for $v_{\rm eff}(r)$, that is expressed in the form of an integral equation for the electron-ion DCF $C_{\rm eI}(r)$:

$$\hat{B}C_{\rm eI}(r) = n_{\rm e}^{0f}(r|v_{\rm eI} - \Gamma_{\rm eI}/\beta - B_{\rm eI}/\beta)/n_0^{\rm e} - 1 - \hat{B}\Gamma_{\rm eI}(r) \ , \tag{2.14}$$

since the effective interionic interaction $v_{\rm eff}(r)$ is given by

$$\beta v_{\rm eff}(Q) \equiv \beta v_{\rm II}(Q) - \frac{|C_{\rm eI}(Q)|^2 n_0^{\rm e} \chi_Q^0}{1 - n_0^{\rm e} C_{\rm ee}(Q) \chi_Q^0} \ . \tag{2.15}$$

Here, $\gamma(r) \equiv \int C(|\mathbf{r} - \mathbf{r}'|) n_0^{\rm I} [g_{\rm II}(r') - 1] d\mathbf{r}'$, and $\hat{B}$ denotes an operator defined by

$$\mathcal{F}_Q[\hat{B}^\alpha f(r)] \equiv (\chi_Q^0)^\alpha \mathcal{F}_Q[f(r)] = (\chi_Q^0)^\alpha \int \exp[i\mathbf{Q} \cdot \mathbf{r}] f(r) d\mathbf{r} \ , \tag{2.16}$$

for an arbitrary real number α, and represents a quantum-effect of the electrons through the density response function χ_Q^0 of the noninteracting electron gas. We can obtain a set of closed integral equations (referred to as the QHNC equation) from Eqs. (2.13)–(2.15) by introducing the following approximations [1]. (1) $B_{\rm eI} \simeq 0$ (the HNC approximation). (2) The bridge function $B_{\rm II}$ of the ion-electron mixture is approximated by that of one-component hard-sphere fluid (modified HNC approximation [23]). (3) An approximate $v_{\rm eI}(r)$ is taken to be Eq. (2.8), where we adopt the Gunnarsson-Lundqvist formula [24] for the exchange-correlation potential $\mu_{\rm XC}(n_0^e)$. (4) $v_{\rm II}(r)$ is taken as a pure Coulombic $Z_{\rm I}^2 e^2/r$. (5) For liquid metals where the electrons can be assumed to be at zero temperature, the electron-electron DCF is approximated by $C_{\rm ee}(Q) \simeq -\beta v_{\rm ee}(Q)[1 - G^{\rm jell}(Q)]$ in terms of the the local-field correction (LFC) $G^{\rm jell}(Q)$ of the jellium model; we have used the LFC proposed by Geldart and Vosko [25] in our many applications to liquid metals.

Under these approximations, a set of integral equations can be solved to determine the electron-ion and ion-ion correlations in a liquid metal together with the ionization and electron bound states. Figure 1 is an applied example of this procedure to liquid metals: the structure factors of liquid rubidium at temperature 313 K and density $1.03 \times 10^{22}/{\rm cm}^3$. The full curve is the QHNC result, which exhibits an excellent agreement with experiments denoted by open circles (neutron-scattering [26]) and full circles (X-ray [27]). From this example, we can expect the QHNC method to yield good results for partially ionized plasmas.

However, when we apply the QHNC method to a plasma, there occur the following problems; the LFC involved in the electron-electron DCF must be evaluated at arbitrary temperature in dealing with a plasma. Although the LFC at the absolute zero temperature

has been calculated by many investigators and applied to many kinds of liquid metals, there is no standard way to calculate the LFC at finite temperature. For this purpose, we adopt the one-component QHNC equation [28] for an electron gas in the uniform positive background to obtain the electron-electron DCF at arbitrary temperature, which is written for an integral equation for the electron-density distribution $n_e(r|e)$ around the fixed electron in an electron gas,

$$n_e(r|e) = n_e^0(r|U_{\rm eff}) = \Sigma_i f(\epsilon_i)|\psi_i(r)|^2 \tag{2.17}$$

with

$$\beta U_{\rm eff}(r) \equiv \beta v_{ee}(r) - \int C_{ee}(|\mathbf{r}-\mathbf{r}'|)[n_e(r'|e) - n_0^e]d\mathbf{r}' \,. \tag{2.18}$$

Here, the DCF for a one-component system is defined by

$$n_0^e C_{ee}(Q) \equiv 1/\chi_Q^0 - 1/\chi_Q^{ee} = -\beta v_{ee}(Q)[1 - G(Q)] \,. \tag{2.19}$$

The Fourier transform of the density distribution yields the following bootstrap relation to determine the DCF $C_{ee}(Q)$ with combined use of Eqs. (2.17) and (2.18):

$$\mathcal{F}_Q[n_e(r|e) - n_0^e] = \chi_Q^{\rm ee}/\chi_Q^0 - 1 = 1/[1 - n_0^e C_{ee}(Q)\chi_Q^0] - 1 \,, \tag{2.20}$$

which is derived from a certain ansatz [28]. At this point, it should be noted that the QHNC equation (2.17) reduces to the well known HNC equation for a classical electron gas in the high temperature limit, because of the relations: $\chi_Q^0 = 1$, $\chi_Q^{\rm ee} = S_{\rm ee}(Q)$ and $n_e^0(r|U_{\rm eff}) = n_0^e \exp[-\beta U_{\rm eff}(r)]$ in the classical limit. As a result, the approximation (5) can be replaced by the one-component QHNC equation (2.17) for the electron gas; with use of other approximations (1)–(4), this replacement makes Eqs (2.13)–(2.15) a closed set of equations for a plasma including a liquid metal as a special case. The electron-ion and the ion-ion RDF's of liquid Rb at 313 K are plotted in Fig. 2 along with the effective ion-ion interactions calculated using both the QHNC and Geldart-Vosko $G(Q)$; the resulting two effective potentials differ with each other, but yield almost the same ion-ion RDF's as shown

by the full curve and open circles. In Fig. 2 the electron-ion RDF obtained from the QHNC method has an inner-core structure which is caused by the orthogonality of the free-electron to the bound-electron wave functions. On the other hand, it should be noticed that the usual liquid-metal theory based on the Ashcroft pseudopotential [29] yields an electron-ion RDF, which has no inner-core structure (shown by full circles). The Ashcroft pseudopotential is constructed by neglect of this inner-core structure; this cut-off of the inner-core structure brings about a simple treatment of liquid metals in the standard liquid-metal theory.

III. NUMERICAL CALCULATION APPLIED TO RUBIDIUM PLASMA

Already, we have calculated the electronic and ionic structures of liquid rubidium in a wide range of temperatures and densities: compressed states [30] and expanded states [31]. To show the applicability of the QHNC method to a plasma state, therefore here we take, as an example, liquid rubidium changing its temperature from 313 K to 3.5×10^5 K (30 eV) at fixed ion-density $r_{\rm s}^{\rm I}=5.388$. Here, $r_{\rm s}^{\rm I}$ denotes the Wigner-Seitz radius $a\equiv r_{\rm s}^{\rm I}a_{\rm B}$ in units of the Bohr radius $a_{\rm B}$.

In the application of the QHNC equation to a plasma, we must calculate the electron-density distribution $n_e^0(r|U_{\rm eff})$ under the external potential $U_{\rm eff}(r)$ to get $g_{\rm eI}(r)$ and $n_{\rm e}(r|{\rm e})$ by solving the wave equation generally. However, it is difficult to determine this density distribution from the wave equation at high temperatures, where it becomes nearly the classical Boltzmann factor: $n_e^0(r|U_{\rm eff}) = \Sigma_i f(\epsilon_i)|\psi_i(r)|^2 \Rightarrow n_0^e \exp[-\beta U_{\rm eff}]$. In the calculation of the free-electron density distribution, $n_e^{0f}(r|U_{\rm eff}) = 2\int f(\epsilon_{\mathbf{p}})|\psi_{\mathbf{p}}(r)|^2 d\mathbf{p}/(2\pi\hbar)^3$, at finite temperature, the electron kinetic energy $\epsilon_{\mathbf{p}}$ is not limited within the Fermi energy $E_{\rm F}$, as is the case at zero temperature. In addition, since the electron-density distribution $n_e^0(r|U_{\rm eff})$ begins to approach the Boltzmann factor from the large distance as the temperature increases, we must calculate the wave functions with large angular momentum l to correctly obtain the classical electron-density distribution in the large distance at high temperature. We can circumvent this difficulty by using the Thomas-Fermi (TF) approximation to the

electron-density distribution for $r > r_{\rm c}$; the distance $r_{\rm c}$ can be chosen according to the temperature so that $n_e^0(r|U_{\rm eff})$ calculated from the wave equation becomes almost equal to the TF result for $r > r_{\rm c}$. This situation can be seen in the following calculation.

The electron-density distribution around a fixed electron is calculated for a partially degenerate electron plasma at the density $2.51 \times 10^{22}/{\rm cm}^3$, that is, $r_{\rm s} = 4$ in terms of $r_{\rm s}a_{\rm B} \equiv (3/4\pi n_0^e)^{1/3}$ defined for the electron density n_0^e; the results calculated for temperatures from 0.05 eV to 30 eV are shown in Fig. 3. The electron degeneracy is denoted by $\theta \equiv k_{\rm B}T/E_{\rm F}$, i.e., the temperature over the Fermi energy. For high degeneracy (0.05 eV), the TF approximation (denoted by full circles) gives quite a different density distribution from the one calculated by the wave equation. When the temperature is increased to 10 eV, the TF result becomes almost same to that obtained by the wave equation except near the origin. When the temperature approaches 30 eV, the electron-electron correlation reduces to the classical one; the classical HNC equation for the one-component plasma (OCP) with the electron plasma parameter $\Gamma_{\rm e} = 0.277$ (30 eV) provides an indistinguishable result from the TF calculation as is shown in Fig. 3 by the dashed curve. Here, the electron plasma parameter is defined by $\Gamma_e \equiv \beta e^2/r_{\rm s}a_{\rm B}$. In the calculation of $n_e(r|e)$, we can obtain at the same time the electron-electron DCF, which determines the LFC $G(Q)$ from the relation $\beta C_{\rm ee}(Q) = -v_{\rm ee}(Q)[1-G(Q)]$; the calculated $G(Q)$ at $r_s = 4$ is shown in Fig. 4 for each temperature corresponding to Fig. 3. This figure indicates that the LFC at high temperature can be approximated by that calculated from the classical HNC for the OCP, as is shown by the case of 30 eV ($\theta = 9.62$), where the LFC of the classical OCP is denoted by the dashed curve. In this way, by means of the QHNC equation for an electron gas we can obtain the electron-electron DCF, which determines the plasma properties in terms of the QHNC $G(Q)$.

Using now the QHNC-LFC $G(Q)$ instead of a Geldart-Vosko [25] type $G(Q)$, we apply Eqs. (2.13)-(2.14) to rubidium at the fixed density of the normal liquid metal; the temperature has been varied from 0 (313 K) to 30 eV in order to investigate how a liquid-metal becomes a plasma. For the purpose to obtain initial data of the ion-core structure and

the electron-ion correlation for the fully self-consistent QHNC method, we take the jellium-vacancy model as a first step. In this model the following two approximations are introduced in the expression for the electron-ion interaction (2.11), that is,

$$\beta U_{\rm eI}^{\rm eff}(r) = \beta v_{\rm eI}(r) - \sum_l \int C_{el}(|\mathbf{r}-\mathbf{r}'|) n_0^l [g_{\rm II}(r')-1] d\mathbf{r}' \ . \tag{3.1}$$

(1) The ion-ion RDF involved above is approximated by the step function: $g_{\rm II}(r) = \theta(r-a)$, and (2) the electron-ion DCF, by a pure Coulomb force: $C_{\rm eI}(r) = -\beta v_{\rm eI}^c(r)$. Then, the problem to determine the electron-ion RDF becomes identical with the problem to determine the electron density distribution around a fixed nucleus at the center of the spherical-vacancy in the jellium background. This model is essentially same to the INFERNO model [5,7] (or the ion-sphere model) introduced by Liberman and also to the neutral-pseudoatom model [15] proposed by Perrot. By solving these integral equations, we can obtain the electron-ion DCF, and the ion-ion effective interaction (2.15) with the combined use of the electron-electron DCF determined by the one-component QHNC equation (2.17). As a consequence, we can obtain initial input data for the fully self-consistent QHNC equations (2.13)–(2.15). After that, this set of integral equations in conjunction with Eqs. (2.17) and (2.18) is solved iteratively by varying the bound-electron number $Z_{\rm B} = \int_0^\infty \rho_{\rm b}(r) d\mathbf{r}$ until the self-consistent condition (2.4), $n_{\rm e}^{\rm b}(r) = \rho_{\rm b}(r)$, is fulfilled.

In the iteration to solve the QHNC equation, we must evaluate also the free-electron density distribution around the nucleus at arbitrary temperature. It has been the standard method [32,33,2,4,7,18] for the calculation of this free-electron density distribution to use the TF approximation in such a way:

$$n_e^{0f}(r|U) \approx 2 \int_{\mathbf{p}^2/2m+U(r)>0} [\exp(-\beta(\mathbf{p}^2/2m+U(r)-\mu_e^0))+1]^{-1} \frac{d\mathbf{p}}{(2\pi\hbar)^3} \equiv n_f^{\rm TF}(r|U) \ . \tag{3.2}$$

In this expression, the integration of $\mathbf{p}$ is limited within the domain $\mathbf{p}^2/2m+U(r) > 0$ to define the free-electron part of the usual TF formula, $n^{\rm TF}(r|U)$, which involves both the bound- and free-electron density distributions. In Fig. 5, the electron-ion RDF's at temperatures of 3.5×10^4 K and 3.5×10^5 K calculated by the QHNC method are shown in comparison

with the results from the TF approximation (3.2). It should be noticed that the TF formula for the free-electron density distribution (3.2) is not a good approximation except for large distances even at a high temperature of 3.5×10^5 K (θ=5.21), while there the total (free and bound) density distribution can be fairly well described by the TF formula. Noting this fact, we can evaluate the free-electron density distribution function $n_e^{0f}(r|U)$ for large distances $r > r_c$ by the value of $n^{\rm TF}(r|U)-n_e^{0b}(r|U)$ using the TF density distribution $n^{\rm TF}(r|U)$ and the bound-electron density distribution $n_e^{0b}(r|U)$ obtained by the wave equation; in the case 3.5×10^5 K, the cut-distance r_c can be chosen to be $0.9a$ as shown by the arrow in Fig. 5. In this way, we can determine the the electron-ion RDF i.e., $n_e^{0f}(r|U)$, by solving the wave equation only for small angular momentum l; it is enough to take the maximum angular momentum $l_{\rm max} = 15$ even for the high temperature region.

The electron-ion RDF's at temperatures of 1 eV and 3 eV are plotted in Fig. 6 along with the ion-ion RDF's and the effective ion-ion interactions. As is shown in Fig. 2, the electron-ion RDF at a temperature of 313 K has distinct inner-core and outer-core parts. Even at a temperature of 1 eV as shown in Fig. 6, this clear distinction remains as characteristic for a liquid metal; the ionization is practically unity and the ion-ion effective interaction is almost the same structure as that of liquid metal at the normal condition, although the ion-ion correlation becomes weak because of the small plasma parameter $\Gamma \equiv Z_{\rm I}^{5/3}\Gamma_e$. Therefore, we can consider that rubidium remains as a liquid-metal state even at 1.16×10^4 K (1 eV). Figure 6 shows that at a temperature of 3 eV the distinction between inner- and outer-core parts near $0.4a$ disappears and that the ionization, now 1.21, has become significant. Because of the disappearance of this distinction between the the inner- and outer-core structures, it is difficult to construct a pseudopotenital in a plasma state. This makes a contrast with a liquid-metal state, where a pseudopotential such as the Ashcroft potential can be used to set up an effective interaction between ions in a liquid metal.

The temperature variation of the electron-ion RDF is shown in Fig 7 for a range from 0 eV to 30 eV. The electron-ion correlation becomes stronger for temperatures up to 10 eV, and turns to become weaker from 10 eV to 30 eV; the distinction between the inner- and outer-

core parts near the point $0.4a$ is gradually disappearing with increasing temperature. On the other hand, the ion-ion RDF's are shown in Fig. 8 for increasing temperatures from 0 eV (313 K) to 30 eV. Also, the effective ion-ion interactions generating the RDF's in Fig. 8 are plotted in Fig. 9, where the open circles denote the screened Debye potential $\exp(-r/D_e)Z_{\rm I}^2e^2/r$ at a temperature of 30 eV (Γ_e=0.277) with $D_e \equiv (4\pi e^2\beta n_0^e)^{1/2}$. We can see that the ion-ion effective potential approach the screened Debye potential as the electron plasma parameter Γ_e becomes small with increasing temperature. The HNC equation for a one-component fluid with the screened Debye potential at a temperature of 30 eV provides the RDF $g_{\rm II}^{\rm SD}(r)$ in fair agreement with the result from the QHNC method for the electron-nucleus mixture; for example, the structure factor at zero wavenumber becomes $S_{\rm II}(0) = 0.18$ from the screened Debye potential, which should be compared with the QHNC result, $S_{\rm II}(0) = 0.16$. This fact suggests that in the high temperature region where $S_{\rm II}(0)$ becomes large, the ion-sphere model (the jellium-vacancy model) can be improved by using the approximation $g_{\rm II}(r) \approx g_{\rm II}^{\rm SD}(r)$ instead of the step function.

Figure 10 shows the temperature variation of the outer-bound levels of an average ion in Rb plasma at the fixed ion-density of normal liquid metal. The 4s- and 4p-bound levels are plotted there corresponding to free atom, 0, 1, 3, 5, 10, 22, and 30 eV, respectively. As the temperature increases, the bound levels become deeper due to the decrease of bound-electron number, which makes the screening effect weak. At temperatures of 22 and 30 eV, new bound levels, 5s and 4d, appear. The occupation number $f(\epsilon_i)$ at the level ϵ_i is written at each level line in Fig. 10. The ionization variation $Z_{\rm I}$ is shown in the top of Fig. 10 as the temperature is increased.

IV. THE SAHA EQUATION IN THE DENSITY-FUNCTIONAL THEORY

The DF theory provides the exact electron-density distribution $n_e(r|U)$ in the nonuniform electron system caused by an external potential $U(r)$; however, it is important to notice

that this exact density distribution $n_e(r|U)$ at finite temperature is only an average density distribution. Consider a nucleus with the atomic number $Z_{\rm A}$ fixed in an electron gas. The effective external potential $U_{\rm eff}(r)$ defined by the DF theory gives an exact expression for the electron density distribution in terms of a density distribution of noninteracting electrons in the form:

$$n_{\rm e}(r|{\rm N}) = n_{\rm e}^0(r|U_{\rm eff}) = n_{\rm e}^{\rm b}(r|{\rm N}) + n_{\rm e}^{\rm f}(r|{\rm N}) \,, \tag{4.1}$$

which defines an average ion with the $Z_{\rm B}$ bound-electrons: $Z_{\rm B} = \int n_{\rm e}^{\rm b}(r|{\rm N}) d\mathbf{r}$. In the realistic system, the ion should have some integer-number of the bound-electrons with fluctuations in time; the number $Z_{\rm B}$ given by the DF theory is only an average value of this bound-electron number over time. The similar situation is found in the ion structure in a nucleus-electron mixture. Here, we investigate the charge population of differently ionized species in a plasma on the basis of the DF theory.

As is discussed in §. II, the average bound-electron number $Z_{\rm B}$ is defined by Eq. (2.5) in the nucleus-electron model based on the DF theory, and the chemical potential $\mu_{\rm e}^0$ is determined by Eq. (2.7). This average bound-electron number $Z_{\rm B}$ in an ion in a plasma can be represented by

$$Z_{\rm B} = \lambda \frac{d}{d\lambda} \ln \Xi_{\rm B} = \sum_{i=1}^{M} \frac{g_i}{\exp[\beta(\epsilon_i - \mu_{\rm e}^0))] + 1} \,, \tag{4.2}$$

if we introduce here the grand partition function $\Xi_{\rm B} \equiv \prod_{i=1}^{M} [1 + \lambda \exp(-\beta\epsilon_i)]^{g_i}$ for the ion with bound-electrons, which have M bound-levels ϵ_i with the degeneracy g_i, and $\lambda \equiv \exp(\beta\mu_e^0)$. Alternatively, the grand partition function $\Xi_{\rm B}$ can be expanded in a polynomial of λ:

$$\Xi_{\rm B} \equiv \prod_{i=1}^{M} [1 + \lambda \exp(-\beta\epsilon_i)]^{g_i} = \sum_{Q=0}^{G} \lambda^Q Z_Q \tag{4.3}$$

with $G \equiv \sum_{i=1}^{M} g_i$. In this expression, the canonical partition function Z_Q of the ion with the Q bound electrons is defined by

$$Z_Q \equiv \sum_l \Omega(E_l^Q) \exp[-\beta E_l^Q] \tag{4.4}$$

$$= \sum_{\sum n_s=Q} \left(\prod_{s=1}^{M} \frac{g_s!}{n_s!(g_s-n_s)!} \right) \exp[-\beta E^Q_{\{n_s\}}] \tag{4.5}$$

$$= \sum_{\sum n_s=Q} \prod_{s=1}^{M} [{}_{g_s}C_{n_s} \exp(-\beta \epsilon_s n_s)] \tag{4.6}$$

with the total energy $E^Q_l \equiv \sum_{i=1}^{M} \epsilon_s n_s = E^Q_{\{n_s\}}$ (n_s=0 or 1) for the Q bound-electrons. Here, $\Omega(E^Q_l)$ represents the number of basic states with the energy E^Q_l for the Q bound-electrons in the ion. Furthermore, the grand partition function $\Xi_{\rm B}$ is written as $\Xi_{\rm B} = \sum_{i=1}^{G} U_Q$ using the function U_Q defined by,

$$U_Q \equiv e^{\beta \mu^0_{\rm e} Q} Z_Q = \sum_{\sum n_s=Q} \prod_{s=1}^{M} \{ \ {}_{g_s}C_{n_s} \exp[\, \beta(\mu^0_{\rm e} - \epsilon_s) n_s \,] \ \} \, . \tag{4.7}$$

From Eqs. (4.3) and (4.7), we obtain the average bound-electron number $Z_{\rm B}$ in another form:

$$Z_{\rm B} = \lambda \frac{d}{d\lambda} \ln \Xi_{\rm B} = \sum_{Q=0}^{G} Q \frac{U_Q}{\Xi_{\rm B}} = < Q > \, , \tag{4.8}$$

which means that the probability for the bound-electron number of the ion to be Q is given by $U_Q/\Xi_{\rm B}$.

From another point of view, let us count the number of ions with the Q bound-electrons in a plasma, which is denoted by N_Q; this satisfies the relation $\sum_{Q=0}^{G} N_Q = N_{\rm I}$ since the total ion number in the system is $N_{\rm I}$. In terms of N_Q, the average bound-electron number $Z_{\rm B}$ is determined by another way:

$$\sum_{Q=0}^{G} Q \frac{N_Q}{N_{\rm I}} = Z_{\rm B} \, . \tag{4.9}$$

The above two expressions of Eqs. (4.9) and (4.8) for the probability that the ion in a plasma has Q bound-electrons give rise to the relation: $N_Q/N_{\rm I} = U_Q/\Xi_{\rm B}$, that is,

$$\frac{N_Q}{U_Q} = \frac{N_{\rm I}}{\Xi_{\rm B}} \, . \tag{4.10}$$

Since the righ-side of this equation is independent of Q, we obtain the expression: $N_Q/U_Q = N_{Q-1}/U_{Q-1}$, which can be rewritten in the form:

$$N_Q/N_{Q-1} = U_Q/U_{Q-1} = \exp[\beta\mu_{\rm e}^0] Z_Q/Z_{Q-1}\,. \tag{4.11}$$

If we introduce the canonical partition function $Z'_Q \equiv \exp[\beta E_0^Q] Z_Q$ using excitation energies E_n^Q–E_0^Q measured from the ground state E_0^Q of the ion with the Q bound-electrons, Eq. (4.11) is rewritten as

$$\frac{N_Q}{N_{Q-1}} = \exp[\beta(\mu_{\rm e}^0 + I_Q)] \frac{Z'_Q}{Z'_{Q-1}} \tag{4.12}$$

with the ionization energy $I_Q \equiv E_0^{Q-1}$–E_0^Q in the ground state. This is the Saha equation, which is applicable to a plasma where the electrons may be degenerate at any degree, and the ions and the electrons in a plasma may interact strongly with each other at high densities. When the temperature of a plasma becomes so high that the electrons behave as classical particles, the electron chemical potential is determined by the classical relation:

$$n_0^e \lambda_e^3/2 = \frac{n_0^e}{Z_e} = \exp[\beta\mu_{\rm e}^0] \tag{4.13}$$

with the canonical partition function $Z_e = 2(2\pi m/h^2\beta)^{3/2}$ of a noninteracting electron gas and the thermal wavelength λ_e. As a result from the above equation, Eq. (4.12) is reduced to the usual expression for the Saha equation [34]:

$$\frac{n_Q}{n_{Q-1} n_0^e} = \exp(\beta I_Q) \frac{Z'_Q}{Z'_{Q-1} Z_e} \tag{4.14}$$

to determine the ion-density $n_Q = N_Q/V$ in the volume V. At this point, note that the fundamental relation (4.10) to derive the Saha equation is nothing but an ansatz introduced by Bar-Shalom *et al.* [35].

It should be recognized here that the solution of the Saha equation, (4.12) or (4.14), is obtained by determining the partition function U_Q of a plasma with aids of the relation (4.10), that is $n_Q = n_0^{\rm I} U_Q/\Xi_{\rm B}$. For this calculation, we can use the following recursive formulas [35,36] for the partition function U_Q of the ion with the Q bound-electrons:

$$U_0 = 1\,, \tag{4.15}$$

$$U_Q = \sum_{n=1}^{Q} \chi_n U_{Q-n}/Q\,, \tag{4.16}$$

where $\chi_n = -\sum_{i=1}^{M} g_i(-X_i)^n$ with $X_i = \exp[-\beta(\epsilon_i - \mu_e^0)]$.

An applied example of our formula to evaluate the ion population $P(Q)$ is shown in the case of Rb plasmas. In the nucleus-electron model based on the DF theory, the bound-levels ϵ_i of the ion in a plasma is determined by solving the wave-equation for the self-consistent potential given by $U_{\rm eI}^{\rm eff}(r)$ (3.1), and the chemical potential μ_e^0 of electrons is evaluated by the condition (2.7); the temperature variation of the bound-levels of Rb plasma was shown in Fig. 10 for a range from 0 eV to 30 eV. Using these values, we can obtain U_Q from the recursive relations, (4.15) and (4.16). In this way, the charge population $P(Q) \equiv U_Q/\Xi_{\rm B}$ is evaluated for Rb plasma with the atomic number $Z_{\rm A}$=37 varying the temperature from 3 eV to 30 eV at fixed ion-density $1.03\times10^{22}/{\rm cm}^3$ ($r_{\rm s}^{\rm I} = 5.388$), as was studies in §. III for the evaluation of the electron-ion and ion-ion RDF's. Figure 11 displays the charge population $P(Q)$ in Rb plasmas for this temperature variation; the bound-electron number $Z_{\rm B}$ from Eq.(4.9) is coincident with the values obtained previously by Eq. (2.5) for each temperature, as a matter of course. At a sufficiently low temperature such as 1 eV, the charge population reduces to $P(Q) = \delta_{Q,36}$ for Rb plasmas at liquid-metal density.

V. CONCLUSIVE DISCUSSION

We have demonstrated that the QHNC method, which has been successfully applied to many kinds of liquid metals, can be extended to treat a partially ionized plasma, taking rubidium as an illustrating example. In the application of the QHNC method to a plasma, it is necessary to use the LFC $G(Q)$ at arbitrary temperature, which is determined by the one-component QHNC equation for an electron gas in the jellium; the QHNC $G(Q)$ reduces to the LFC obtained by the classical HNC for the OCP at high temperatures as is shown in Fig. 4. In the numerical calculation in the QHNC method for a plasma, it is very time-consuming to evaluate free-electron density distributions at high temperatures; this problem can be easily circumvented by combined use of the TF approximation as discussed in §. III. However, the simple TF approximation to the free-electron density distribution is shown to

give only a rough estimation in Fig. 5; this may not be applied to calculate the accurate atomic structure in a plasma, although there are many examples as mentioned before.

In a liquid metal, the electron-ion RDF has a clear inner-core structure distinct from outer-core structure (cf. Fig. 2); this distinction enables us to construct a pseudopotential in a liquid liquid metal. In the case of Rb, it remains as a liquid metal even at a temperature of 1.16×10^4 K where the inner- and outer-core distinction is clearly seen with $Z_{\rm I}=1$ as is displayed in Fig. 6; this distinction disappears at 3 eV, where rubidium becomes a plasma with a significant ionization $Z_{\rm I}=1.21$.

It is important to remember that the ion-sphere (IS) model is not an appropriate approximation to treat a high-temperature plasma with a small plasma-parameter Γ. In the IS model, the ion-ion RDF is approximated by the step function with the Wigner-Seitz radius a. Therefore, this approximation is only valid in the strongly correlated region, where the structure factor $S_{\rm II}(0)\approx0$ at zero wavenumber, because of the relation:

$$-n_0^{\rm I}\int[g_{\rm II}(r)-1]d\mathbf{r}=1-S_{\rm II}(0)\approx n_0^{\rm I}4\pi a^3/3\equiv1\ . \tag{5.1}$$

This condition is very important to keep charge neutrality around the ion [37]:

$$Z_{\rm I}=-Z_{\rm I}n_0^{\rm I}\int[g_{\rm II}(r)-1]d\mathbf{r}+n_0^{\rm e}\int[g_{\rm eI}(r)-1]d\mathbf{r}\,. \tag{5.2}$$

When the ion-ion RDF becomes weaker as the temperature increases, the structure factor $S_{\rm II}(0)$ grows large; there, the IS model is not properly applicable. This situation is exemplified in our calculation of the ionization $Z_{\rm I}$. The IS (jellium-vacancy) model provides the ionization $Z_{\rm I}$: 1.27, 2.05, 3.80, 5.28 and 6.55 for temperatures: 3, 5, 10, 22, and 30 eV, respectively, while the corresponding values from the fully self-consistent QHNC calculation are 1.21, 1.96, 3.71, 5.08 and 6.08, respectively. We can see that significant differences are manifested between the IS and QHNC results, as the temperature increases. The reason for these differences can be ascribed to the fact that the IS model produces a screening effect from the ions contained in Eq. (5.2) in the approximated form $Z_{\rm I}[1-S_{\rm II}(0)]\approx Z_{\rm I}$, which becomes too strong for a plasma at high temperatures where $S_{\rm II}(0)$ becomes large. As a

consequence, the neutral-atom model [15] based on the IS model is, also, not appropriate to construct an effective ion-ion interaction at a high-temperature plasma. As discussed in §.III, the IS model can be improved by using the ion-ion RDF from the HNC equation for a screened Debye potential instead of the step function, in dealing with a high-temperature plasma.

In the QHNC method, the inner-structure (the atomic structure of the ion) is determined in the consistent way with the outer structures (the electron-ion and ion-ion RDF's and the average ionization $Z_{\rm I}$). Therefore, we can expect this method to provide an accurate procedure to deal with the atomic structure in a high-density plasma; the bound-levels in an ion can be calculated by taking account of the density and temperature effects as is shown in Fig. 10. In addition, it should be remarked that the DF theory leads to the Saha equation as discussed in §. IV, and the QHNC method based on the DF theory can provide a procedure to solve the Saha equation with ease by using the recursive formula. As an applied example of this formula, the charge population $P(Q)$ is calculated from the QHNC result for a Rb plasma, as is displayed in Fig. 11. Moreover, we can expect that the QHNC method can solve various kinds of problems associated with the atomic structure in a plasma by taking account of the plasma effects. For example, with the combined use of Slater's transition-state method [38], we have already calculated the shift-variation of the K-edge [39] in an aluminum plasma along the shock Hugoniot in good agreement with the experiment performed by DaSilva *et al.* [40].

The QHNC method can provide an accurate description of the metallic system for a wide range of densities and temperatures from the liquid-metal to the plasma state in a unified manner, as is ascertained from many experiments on liquid metals. This fact indicates that the QHNC method can be used to calculate transport properties and equation of state in a wide region from the liquid-metallic to the plasma state, where there has been no systematic applicable theory up to the present.

With decreasing temperature or increasing pressure of a plasma, some bound state of each ion in a liquid metal or plasma begins to disappear into the continuum; it becomes

a narrow-resonant state and disappears gradually as a wide resonance in the continuum. In our calculation of plasma states we do not take account of resonant states. In practice, the resonant-state contribution in a plasma is not as significant as in the case of a liquid metal such as a transition metal. A precise definition of a resonant state [41] is given by the pole $\widetilde{E}_{n\ell}$ of the S-matrix $S_\ell(E)$ concerning the wave equation for an electron under the effective potential (2.2) with $S_\ell(E) = \exp(2i\delta_\ell(E))$ for phase shifts $\delta_\ell(E)$. In a strict way, it is required [1] that the "bound"-electron number $Z_{\rm B}$ in an ion should include a contribution of the physical resonant states ($|\Im m\widetilde{E}_{n\ell}| \ll \Re e\widetilde{E}_{n\ell}$) in addition to the bound electrons with $\epsilon_i < 0$ in such a way that

$$Z_{\rm B} \equiv \sum_{\epsilon_i<0} f(\epsilon_i) + \sum_{n\ell\in\text{phys.res.}} 2(2\ell+1)\Re e[F(\widetilde{E}_{n\ell})] \ . \tag{5.3}$$

In the above, $F(\widetilde{E}_{n\ell})$ is the function introduced by More [42] with the definition:

$$F(\widetilde{E}_{n\ell}) \equiv \frac{1}{i\pi}\int_0^\infty \left(\frac{E}{\widetilde{E}_{n\ell}}\right)^{1/2} \frac{f(E)}{E-\widetilde{E}_{n\ell}} dE \ , \tag{5.4}$$

to represent the thermal occupation probability of a resonant state $\widetilde{E}_{n\ell}$. Also, the chemical potential $\mu_{\rm e}^0$ in consideration of the resonant states should be determined by

$$\begin{aligned} Z_{\rm A} = &\sum_{\epsilon_i<0} \frac{1}{\exp[\beta(\epsilon_i-\mu_{\rm e}^0)]+1} + \sum_{n\ell\in\text{phys.res.}} 2(2\ell+1)\Re e[F(\widetilde{E}_{n\ell})] \\ &+\frac{1}{n_0^{\rm I}}\int \frac{2}{\exp[\beta(p^2/2m-\mu_{\rm e}^0)]+1}\frac{d\mathbf{p}}{(2\pi\hbar)^3} \ . \end{aligned} \tag{5.5}$$

However, the determination of the charge occupation $P(Q)$ taking account of the resonant-state contribution is a problem which remains to be investigated.

Molecular-dynamics (MD) simulation is necessary to study complex systems which are inhomogeneous or time dependent and so on. In the MD simulation of a dense plasma, the Coulomb interactions among close and distant particles must be calculated precisely and efficiently; the Particle-Particle Particle-Mesh (PPPM) method [43,44] should be used in the simulation code to treat many particles. In the particle-particle method the Coulomb forces among close particles are directly summed up and in the particle-mesh method the forces on a particle are interpolated from electric fields at mesh points. In the SCOPE (Strongly

COupled Plasma ParticlE) code [44–46] based on the PPPM method, the Deutsch potential [47] is adopted to imitate quantum effects. With use of the code, bremsstrahlung emission [45], transport coefficients and the Lyapunov exponents [46] were obtained in dense plasmas. However, the applicability of the Deutsch potential is limited to a hydrogen plasma or to a fully ionized plasma at most, since the ion structure is not considered in the derivation of the Deutsch potential. In order to perform a classical MD simulation (SCOPE) on a partially ionized plasma, we must introduce effective classical potentials $v_{ij}^c(r)$ applicable to partially ionized ions in a plasma as a classical mixture of ions and electrons; the QHNC method can produce these effective potentials as follows. The quantum effects of electron-electron interaction can be taken into account by defining an effective classical pair-potential $v_{\rm ee}^c(r)$ between electrons in such a way that the HNC equation for $n_e^c(r|e) = n_0^e g_{\rm ee}^c(r)$ in classical fluids with $v_{\rm ee}^c(r)$ provides the same electron-density distribution $n_e^{\rm QHNC}(r|e)$ determined by the one-component QHNC equation (2.17); this condition is written in the following integral equation for $v_{\rm ee}^c(r)$,

$$n_e^c(r|e) \equiv n_0^e \exp[-\beta v_{\rm ee}^c(r) + \gamma^c(r)] = n_e^{\rm QHNC}(r|e) \tag{5.6}$$

with $\gamma^c(r) \equiv \int C_{\rm ee}^c(|\mathbf{r}-\mathbf{r}'|)[n_e^c(r'|e) - n_0^e] d\mathbf{r}'$. In a similar way, an electron-ion classical potential $v_{\rm eI}^c(r)$ is determined by the condition that the classical electron-ion RDF $g_{\rm eI}^c(r)$ should be identical with the QHNC result:

$$g_{\rm eI}^c(r) \equiv \exp[-\beta v_{\rm eI}^c(r) + \Gamma_{\rm eI}^c(r)] = g_{\rm eI}^{\rm QHNC}(r) \tag{5.7}$$

with

$$\Gamma_{\rm eI}^c(r) \equiv \int C_{\rm ee}^c(|\mathbf{r}-\mathbf{r}'|) n_0^{\rm e} [g_{\rm eI}^c(r') - 1] d\mathbf{r}' + \int C_{\rm eI}^c(|\mathbf{r}-\mathbf{r}'|) n_0^{\rm I} [g_{\rm II}^{\rm QHNC}(r') - 1] d\mathbf{r} \ . \tag{5.8}$$

With use of the effective potentials determined above, the SCOPE code can be applied to investigate dynamical problems in a partially ionized plasma as a classical ion-electron mixture.

We have shown that the QHNC method is extended to treat a *partially ionized* plasma in a wide range of densities and temperatures, and provides the average ionization, the

electron-ion and ion-ion RDF's, the atomic structure of the ions and the charge population of differently ionized species in a self-consistent manner from the atomic number as the only input data. Therefore, this method produces the fundamental quantities necessary to calculate the plasma properties, and offers a procedure to treat the spectroscopic problem in a plasma. It should be kept in mind that the QHNC method can provide a precise description of "simple" plasma where the bound states are clearly distinguished from the continuum state; to take into account the resonant states in a plasma, some improvement is necessary as was discussed in the previous work [1].

ACKNOWLEDGMENTS

J.C. would like to thank Dr. F. Perrot for providing his accurate subroutines necessary for our extension of the QHNC code to treat a plasma.

REFERENCES

[1] J. Chihara, J. Phys.: Condens. Matter **3**, 8715 (1991).

[2] B. F. Rozsnyai, Phys. Rev. A **5**, 1137 (1972).

[3] D. A. Liberman, Phys. Rev. B **20**, 4981 (1979).

[4] S. Skupsky Phys. Rev. A **21**, 1316 (1980).

[5] D. A. Liberman, J. Quant. Spectrosc. Radiat. Transfer, **27**, 335 (1982).

[6] R. M. More, K. H. Warren, D. A. Young and G. B. Zimmerman, Phys. Fluids **31**, 3059 (1988).

[7] B. F. Rozsnyai, Phys. Rev. A **43**, 3035 (1991).

[8] M. W. H. Dharma-wardana and F. Perrot, Phys. Rev. A **26**, 2096 (1982).

[9] J. Chihara, Phys. Rev. A **44**, 1247 (1991).

[10] J. Chihara, Phys. Rev. A **40**, 4507 (1989).

[11] M. Ishitobi and J. Chihara, J. Phys.: Condens. Matter **4**, 3679 (1992).

[12] M. Ishitobi and J. Chihara, J. Phys.: Condens. Matter **5**, 4315 (1993).

[13] J. Chihara and S. Kambayashi, J. Phys.: Condens. Matter **6**, 10221 (1994).

[14] S. Kambayashi and J. Chihara, Phys. Rev. E **53**, 6253 (1996).

[15] F. Perrot, Phys. Rev. A **42**, 4871 (1990).

[16] L. E. González, D. J. González and K. Hoshino, J. Phys.: Condens. Matter **5**, 9261 (1993).

[17] L. E. González, A. Meyer, M. P. Inigues, D. J. González and M. Silbert, Phys. Rev. E **47**, 4120 (1993).

[18] H. Furukawa and K. Nishihara, Phys. Rev. E **46**, 6596 (1992); H. Furukawa, Phys. Rev. E **52**, 2988 (1995).

[19] H. Xu and J. P. Hansen, Phys. Rev. E **57**, 211 (1998).

[20] J. Chihara, Phys. Rev. A **33**, 2575 (1986).

[21] J. Chihara, J. Phys. C: Solid State Phys. **17**, 1633 (1984).

[22] J. Chihara, J. Phys. C: Solid State Phys. **18**, 3103 (1985).

[23] Y. Rosenfeld, J. Stat. Phys. **42**, 437 (1986).

[24] O. Gunnarsson and B. I. Lundqvist, Phys. Rev. B **13**, 4274 (1976).

[25] D. J. W. Geldart and S. H. Vosko, Can. J. Phys. **44**, 2137 (1966).

[26] J. R. D. Copley and S. W. Lovesey, *Int. Phys. Conf. Ser.* **30**, 575 (1979).

[27] Y. Waseda, *The Structure of Non-Crystalline Materials*, (McGrow-Hill, New York, 1980).

[28] J. Chihara and S. Sasaki, Prog. Theor. Phys. **62**, 1979 (1979).

[29] N. W. Ashcroft, Phys. Letter **23**,48 (1966).

[30] J. Chihara and G. Kahl, Phys. Rev. B **58**, 5314 (1998).

[31] J. Chihara and G. Kahl, *Strongly Coupled Coulomb Systems*, edited by G. J. Kalman, K. Blagoev, and J. M. Rommel, (Plenum, New York, 1998), p. 129.

[32] J. C. Stewart and K. D. Pyatt Jr, Astrophys. J. **144**, 1203 (1966).

[33] R. Ying and G. Kalmann, Phys. Rev. A **40**, 3927 (1989).

[34] R. D. Cowan, *Theory of Atomic Spectra*, (University of California Press, Berkeley, 1981).

[35] A. Bar-Shalom, J. Oreg, W. H. Goldstein, D. Shvarts and A. Zigler, Phys. Rev. A **40**, 3183 (1989)

[36] T. Blenski, A. Grimaldi and F. Perrot, Phys. Rev. E **55**, R4889 (1997).

[37] J. Chihara, J. Phys.: Condens. Matter **2**, 8525 (1990).

[38] J. C. Slater, *The self-consistent field for molecules and solids*, (McGraw-Hill, New York, 1974).

[39] J. Chihara, K. Kiyokawa and T. Utsumi (to be publised).

[40] L. DaSilva, A. Ng, B. K. Godwal, G. Chiu, F. Cottet, M. C. Richardson, P. Jaanimagi and Y. T. Lee, Phys. Rev. Letters **62**, 1623 (1989).

[41] R. G. Newton, J. Math. Phys. **1**, 319 (1960).

[42] R. M. More, *Adv. Atom. and Mol. Phys.* **21** 305–56 (1985).

[43] R. W. Hockney and J. W. Eastwood, *Computer Simulation using Particles*, (McGraw-Hill, New York, 1981).

[44] K. Nishihara, Kakuyugo Kenkyu **66**, 253 (1991).

[45] H. Furukawa and K. Nishihara, Phys. Rev. A **42**, 3532 (1990).

[46] Y. Ueshima, K. Nishihara, D. M. Barnett, T. Tajima and H. Furukawa, Phys. Rev. Letters **79**, 2249 (1997).

[47] C. Deutsch, Phys. Letter **60**A, 317 (1977).

FIGURES

FIG. 1. Ion-ion structure factor $S_{\rm II}(Q)$ for liquid Rb at a temperature of 313 K; the QHNC method yields a structure factor (full curve) in excellent agreement with experiments (open [26] and full circles [27]).

FIG. 2. The electron-ion and ion-ion RDF's with the effective interactions in liquid Rb at 313 K. The solid curves denote the RDF's, the total electron-density distribution and the effective ion-ion interaction calculated by using the QHNC $G(Q)$. The dashed curve designates the effective ion-ion potential based on the Geldart-Vosko $G(Q)$, which yields the ion-ion RDF plotted by the open circles; $\bullet$, the electron-ion RDF derived by using an Ashcroft potential.

FIG. 3. Electron-electron correlations in an electron gas at the density of $r_{\rm s}=4$ for temperatures ranging from 0.05 to 30 eV with $\theta \equiv k_{\rm B}T/E_{\rm F}$ indicating the electron degeneracy. The solid curves are calculated by the one-component QHNC equation, while the full circles denote the result from the TF approximation for each temperature. The classical HNC equation for the OCP corresponding to a temperature of 30 eV provides the electron-electron correlation plotted by the dashed curve ("OCP"), which is indistinguishable from the TF result at a temperature of 30 eV.

FIG. 4. The local-field corrections (LFC) at temperatures from 0 to 30 eV determined by the one-component QHNC equation. The LFC calculated by the classical HNC for the OCP with $\Gamma_e=0.227$ is displayed by the dashed curve, which indicates that this can be used to approximate the QHNC LFC at this temperature.

FIG. 5. The electron-ion RDF's calculated from the wave equation and the TF approximation at temperatures of 3.5×10^4 K (3 eV) and 3.5×10^5 K (30 eV). The solid curves denote the results from the wave equation and the dashed curves, from the TF approximation. The TF approximation can not give a good description of the free-electron density distribution $n_e^{\rm f}(r|{\rm I}) = {\rm n}_0^{\rm e}{\rm g}_{\rm eI}({\rm r})$ in the core-region even at a high temperature (30 eV), where the total (bound and free) electron-density distribution is fairly well described by the TF approximation. The electron-ion RDF can be approximated by the TF formula for larger distances than the point (0.9) denoted by the arrow.

FIG. 6. The electron-ion and ion-ion RDF's together with the effective ion-ion interaction at temperatures of 1eV and 3 eV. The electron-ion RDF at 1 eV has an inner-core structure similar to the RDF of a liquid state at the normal condition (cf. Fig. 2), and this inner-core structure near $r/a = 0.4$ disappears at 3 eV with a significant ionization $Z_{\rm I} = 1.21$.

FIG. 7. The temperature dependence of the electron-ion RDF for a range from 0 to 30 eV. The inner-core structure near 0.12 reflects the variation of the bound-electron wave functions in an ion due to the orthogonality between the free- and bound-electron wave functions.

FIG. 8. The temperature dependence of the ion-ion RDF for a range from 0 eV (313 K) to 30 eV. The ion-ion RDF becomes small at 1 eV; nevertheless rubidium remains as a liquid state with $Z_{\rm I} = 1$.

FIG. 9. The temperature dependence of the effective ion-ion interaction for a range from 0 eV (313 K) to 30 eV. The effective potential at a temperature of 30 eV approaches the screened Debye potential denoted by the open circles.

FIG. 10. The temperature variation of outer bound levels (4s, 4p, 4d and 5s) in the Rb ion in a plasma for a range from 0 eV to 30 eV at a fixed density of $r_{\rm s}^{\rm I} = 5.388$. The bound levels become shallow when free atoms are compressed to be a liquid state (0 eV), and turn to become deeper as the temperature is increased with the fixed ion-density. Numbers attached to bound levels denote the occupation numbers $f(\epsilon_i)$, and the ionization $Z_{\rm I}$ for each temperature is written in the top of this figure.

FIG. 11. The dependence of the charge population $P(Q)$ on the temperature varying from 3 eV to 30 eV for Rb plasma ($Z_{\rm A}$=37) at a fixed ion-density of $1.03\times10^{22}/{\rm cm}^3$ ($r_{\rm s}^{\rm I} = 5.388$). This charge population provides the average bound-electron $Z_{\rm B}$ of ion, as denoted in this figure for each temperature along with the ionization $Z_{\rm I} \equiv Z_{\rm A} - Z_{\rm B}$.

Figures

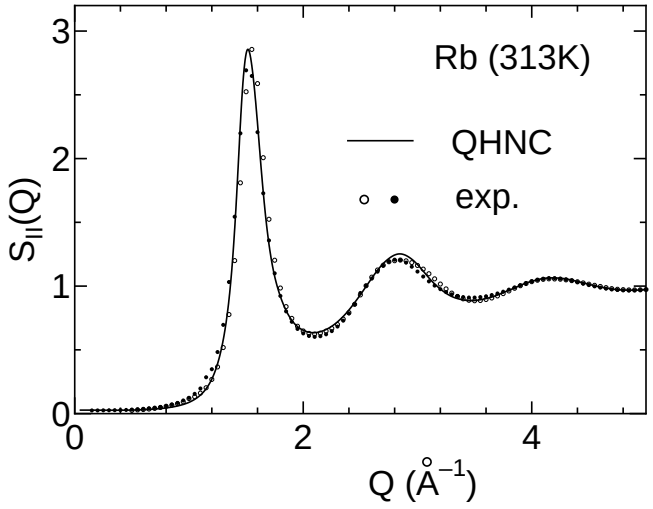

FIG. 1. Ion-ion structure factor $S_{\rm II}(Q)$ for liquid Rb at a temperature of 313 K; the QHNC method yields a structure factor (full curve) in excellent agreement with experiments (open [26] and full circles [27]).

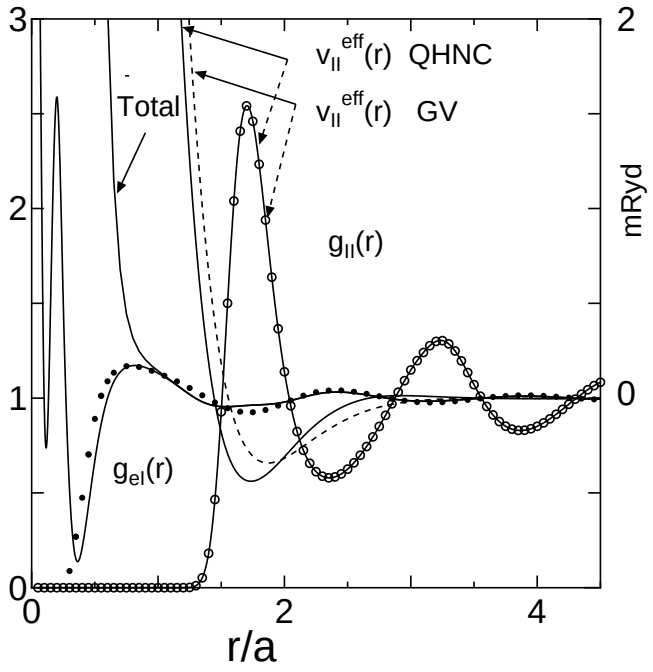

FIG. 2. The electron-ion and ion-ion RDF's with the effective interactions in liquid Rb at 313 K. The solid curves denote the RDF's, the total electron-density distribution and the effective ion-ion interaction calculated by using the QHNC $G(Q)$. The dashed curve designates the effective ion-ion potential based on the Geldart-Vosko $G(Q)$, which yields the ion-ion RDF plotted by the open circles; •, the electron-ion RDF derived by using an Ashcroft potential.

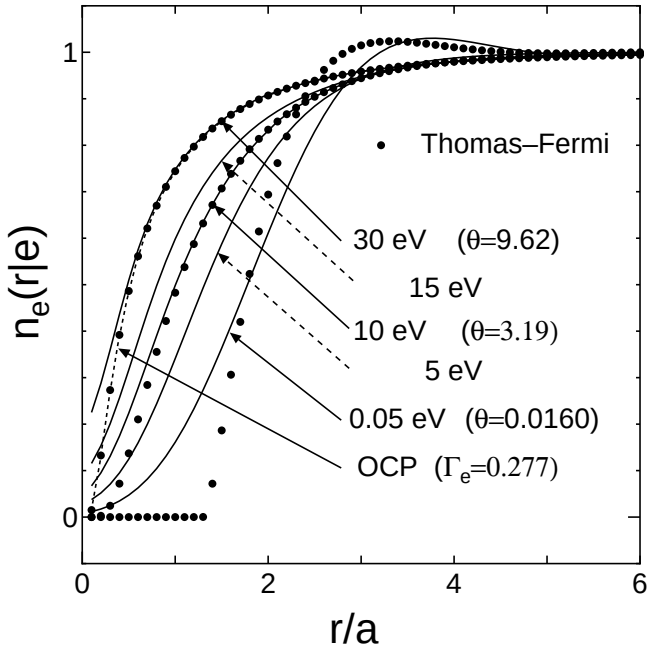

FIG. 3. Electron-electron correlations in an electron gas at the density of $r_s = 4$ for temperatures ranging from 0.05 to 30 eV with $\theta \equiv k_{\rm B}T/E_{\rm F}$ indicating the electron degeneracy. The solid curves are calculated by the one-component QHNC equation, while the full circles denote the result from the TF approximation for each temperature. The classical HNC equation for the OCP corresponding to a temperature of 30 eV provides the electron-electron correlation plotted by the dashed curve ("OCP"), which is indistinguishable from the TF result at a temperature of 30 eV.

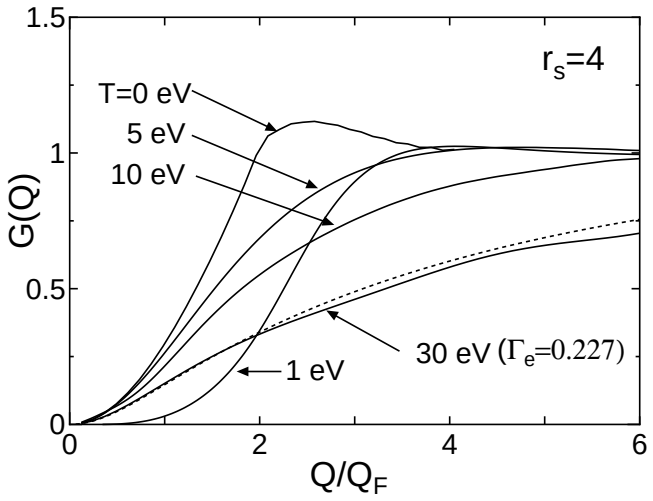

FIG. 4. The local-field corrections (LFC) at temperatures from 0 to 30 eV determined by the one-component QHNC equation. The LFC calculated by the classical HNC for the OCP with $\Gamma_e = 0.227$ is displayed by the dashed curve, which indicates that this can be used to approximate the QHNC LFC at this temperature.

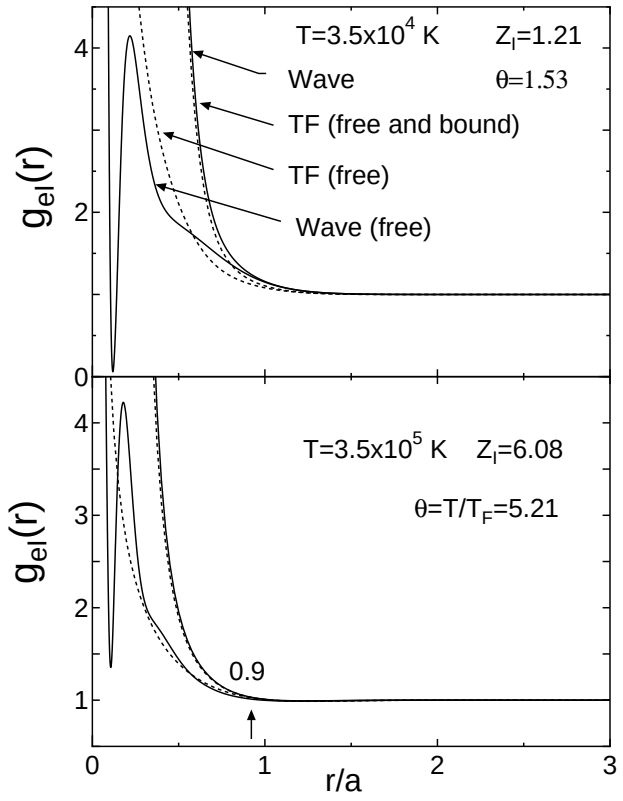

FIG. 5. The electron-ion RDF's calculated from the wave equation and the TF approximation at temperatures of 3.5×10^4 K (3 eV) and 3.5×10^5 K (30 eV). The solid curves denote the results from the wave equation and the dashed curves, from the TF approximation. The TF approximation can not give a good description of the free-electron density distribution $n_e^{\rm f}(r|{\rm I}) = {\rm n}_0^{\rm e}{\rm g}_{\rm eI}({\rm r})$ in the core-region even at a high temperature (30 eV), where the total (bound and free) electron-density distribution is fairly well described by the TF approximation. The electron-ion RDF can be approximated by the TF formula for larger distances than the point (0.9) denoted by the arrow.

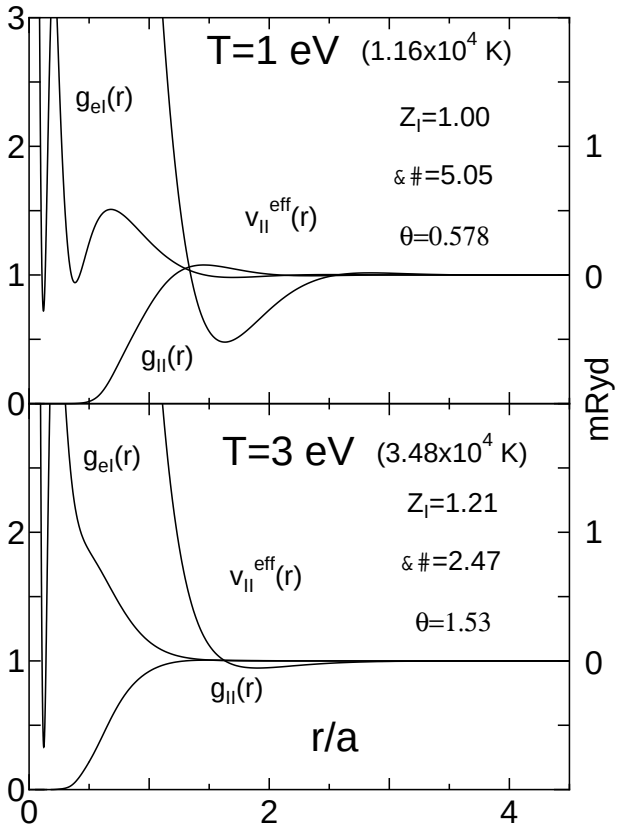

FIG. 6. The electron-ion and ion-ion RDF's together with the effective ion-ion interaction at temperatures of 1eV and 3 eV. The electron-ion RDF at 1 eV has an inner-core structure similar to the RDF of a liquid state at the normal condition (cf. Fig. 2), and this inner-core structure near $r/a = 0.4$ disappears at 3 eV with a significant ionization $Z_{\rm I} = 1.21$.

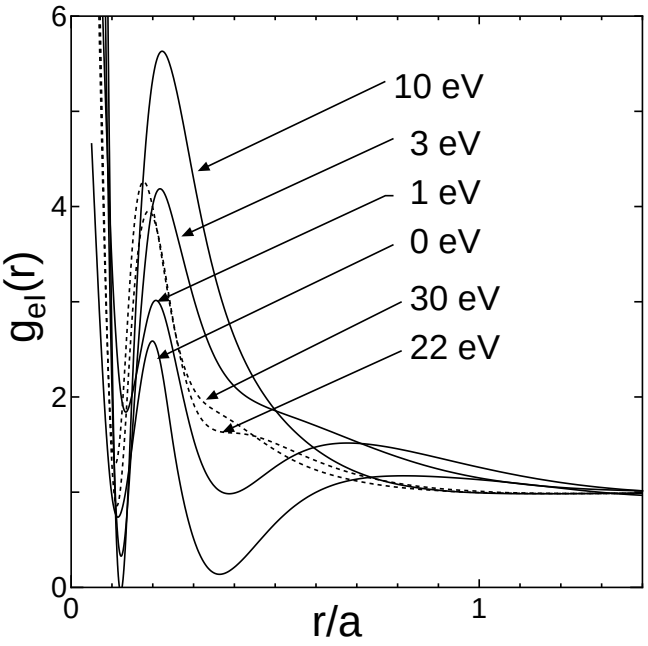

FIG. 7. The temperature dependence of the electron-ion RDF for a range from 0 to 30 eV. The inner-core structure near 0.12 reflects the variation of the bound-electron wave functions in an ion due to the orthogonality between the free- and bound-electron wave functions.

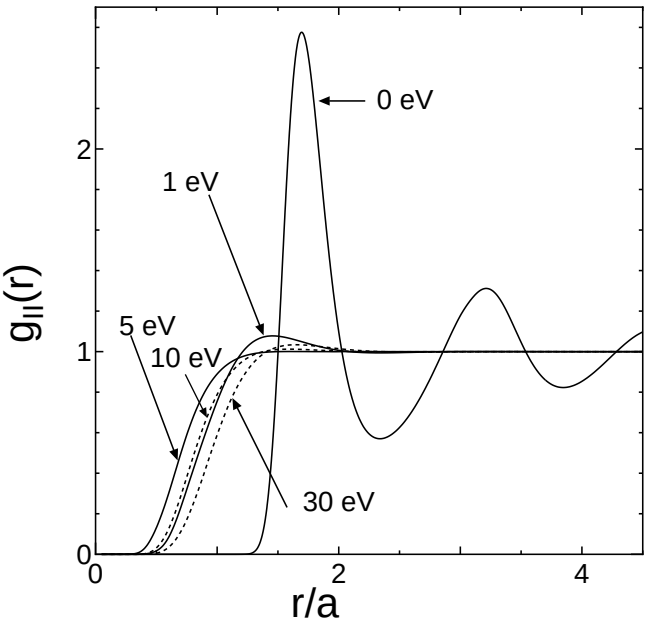

FIG. 8. The temperature dependence of the ion-ion RDF for a range from 0 eV (313 K) to 30 eV. The ion-ion RDF becomes small at 1 eV; nevertheless rubidium remains as a liquid state with $Z_I = 1$.

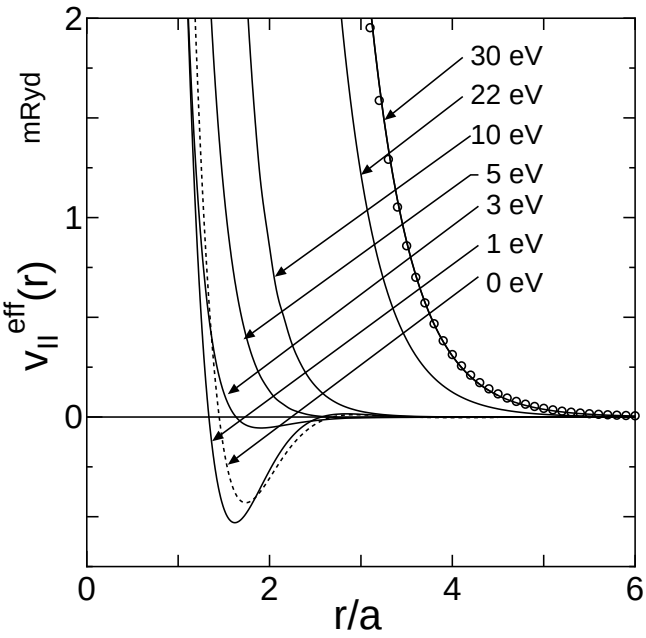

FIG. 9. The temperature dependence of the effective ion-ion interaction for a range from 0 eV (313 K) to 30 eV. The effective potential at a temperature of 30 eV approaches the screened Debye potential denoted by the open circles.

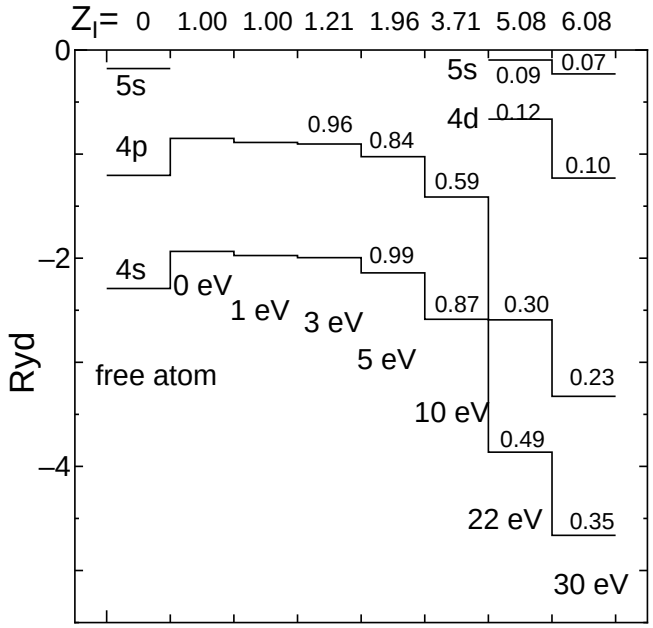

FIG. 10. The temperature variation of outer bound levels (4s, 4p, 4d and 5s) in the Rb ion in a plasma for a range from 0 eV to 30 eV at the fixed density of $r_s^{\rm I} = 5.388$. The bound levels become shallow when free atoms are compressed to be a liquid state (0 eV), and turn to become deeper as the temperature is increased with the fixed density. Numbers attached to bound levels denote the occupation numbers $f(\epsilon_i)$, and the ionization $Z_{\rm I}$ for each temperature is written in the top of this figure.

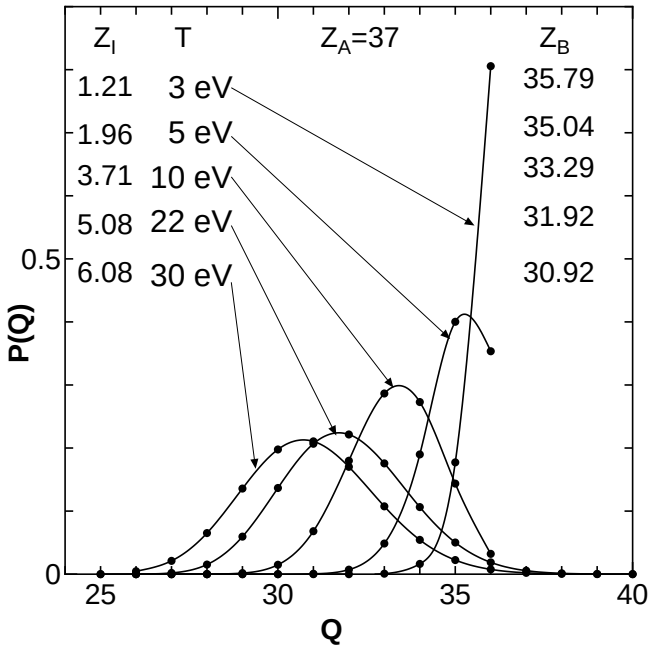

FIG. 11. The dependence of the charge population $P(Q)$ on the temperature varying from 3 eV to 30 eV for Rb plasma ($Z_{\rm A}$=37) at the fixed density of $1.03\times10^{22}/{\rm cm}^3$ ($r_s^{\rm I}=5.388$). This charge population provides the average bound-electron $Z_{\rm B}$ of ion, as denoted in this figure for each temperature along with the ionization $Z_{\rm I}\equiv Z_{\rm A}-Z_{\rm B}$.